

Controlling the cation distribution and electric polarization with epitaxial strain in Aurivillius-phase $\text{Bi}_5\text{FeTi}_3\text{O}_{15}$

Axiel Yaël Birenbaum* and Claude Ederer†

Materials Theory, ETH Zürich, Wolfgang-Pauli-Strasse 27, 8093 Zürich, Switzerland

(Dated: May 13, 2022)

This work explores the impact of in-plane bi-axial (epitaxial) strain on the cation distribution and electric polarization of the Aurivillius-phase compound $\text{Bi}_5\text{FeTi}_3\text{O}_{15}$ using first-principles electronic structure calculations. Our calculations indicate that the site preference of the Fe^{3+} cation can be controlled via epitaxial strain. Tensile strain enhances the preference for the *inner* sites within the perovskite-like layers of the Aurivillius-phase structure, whereas compressive strain favors occupation of the *outer* sites within the perovskite-layers, i.e., the sites close to the Bi_2O_2 layer. Controlling the distribution of the magnetic cations offers the possibility to control magnetic order in this magnetically dilute system. Furthermore, the magnitude of the electric polarization is strongly strain-dependent, increasing under tensile strain and decreasing under compressive strain. Analysis of the Born effective charges reveals strongly anomalous charges, both of the Bi^{3+} cations and the Ti^{4+} cations.

Controlling the properties of complex transition metal oxides by epitaxial strain, i.e., by growing thin films of a certain material on a substrate with specific lattice mismatch, has emerged as a very efficient way for designing optimized functionalities.¹ In particular, the effect of epitaxial strain on the ferroelectric properties of perovskite materials is well studied,² and dramatic enhancements of polarization and ferroelectric ordering temperatures,³ as well as emergence of ferroelectricity in otherwise nonpolar materials have been reported.^{4,5}

Recently, layered perovskite-related systems have come into focus as being potentially more amenable to developing polar lattice distortions compared to bulk perovskites.⁶ Examples include artificial perovskite superlattices and double perovskites, as well as several families of naturally-layered perovskite-derived crystal structures such as the Ruddlesden-Popper series, Aurivillius-phases, or Dion-Jacobson systems. Only few studies addressing the strain response of these naturally-layered materials are currently available. Such studies are, however, of great interest due to the different mechanism underlying the ferroelectricity in these systems. A different mechanism could lead to a different strain response compared to bulk perovskite ferroelectrics.

Here we study the case of $\text{Bi}_5\text{FeTi}_3\text{O}_{15}$,^{7,8} which is a representative of the family of naturally-layered Aurivillius-phases, and is of particular interest due to its potential multiferroic properties.⁹ The crystal structure of the Aurivillius-phases consists of m perovskite layers ($\text{A}_{m-1}\text{B}_m\text{O}_{3m+1}$)²⁻ stacked periodically along the [001] direction, and separated by fluorite-like $(\text{Bi}_2\text{O}_2)^{2+}$ layers (see Fig. 1).^{10,11} $\text{Bi}_5\text{FeTi}_3\text{O}_{15}$ corresponds to the case with $m = 4$.

A previous first-principles study of polarization-strain coupling in the $m = 3$ Aurivillius compound $\text{Bi}_4\text{Ti}_3\text{O}_{12}$ has shown a large response of in-plane polarization under bi-axial strain.¹³ Apart from the introduction of an additional perovskite layer and the presence of the nominally non-ferroelectric Fe^{3+} cation, an important additional degree of freedom in $\text{Bi}_5\text{FeTi}_3\text{O}_{15}$ compared to

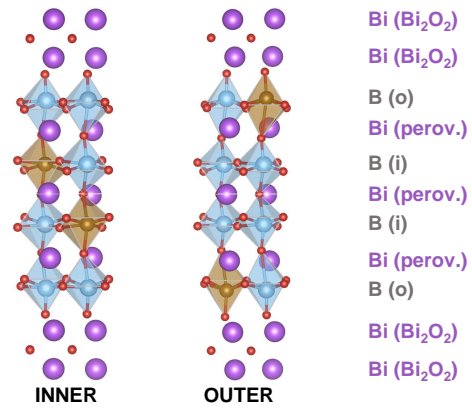


FIG. 1. (Color online) The two B -site cation distributions used in this work, the *inner* and *outer* configurations. Sites occupied with Fe (Ti) are indicated as brown (blue) spheres with corresponding coordination octahedra; Bi (O) ions are shown as purple (red) spheres. Labels for the cations in the different layers (which are used for the discussion of the Born effective charges) are listed on the right. This figure was constructed using VESTA.¹²

$\text{Bi}_4\text{Ti}_3\text{O}_{12}$ is the distribution of Fe^{3+} and Ti^{4+} cations over the available B sites within the perovskite layers of the Aurivillius structure. While the $\text{Fe}^{3+}/\text{Ti}^{4+}$ cations do not tend to form an ordered arrangement, a preferential occupation of the inner perovskite site with Fe has been reported experimentally¹⁴ and confirmed recently by density functional theory (DFT) calculations.⁹ The cation distribution can in principle influence properties such as electric polarization or the likelihood and character of magnetic order, and it could also affect the strain response of the material. Furthermore, a systematic variation of the relaxed lattice constants with the distribution of Fe over the inner/outer perovskite layers has been found in Ref. 9, suggesting that it might be possible to influence the cation distribution by epitaxial strain.

Here, we verify this hypothesis and study the effect of strain on the cation distribution and on the result-

ing electric polarization of $\text{Bi}_5\text{FeTi}_3\text{O}_{15}$. We focus on two representative configurations depicted in Fig. 1, one with all Fe sitting in the *outer* perovskite layers and one with all Fe sitting in the *inner* perovskite layers. Both configurations lower the experimentally observed $A2_1am$ space group symmetry to monoclinic $P2_1$. We note that these two configurations represent the only possibilities to distribute Fe and Ti within the minimal unit cell of the $A2_1am$ structure (containing 2 formula units of $\text{Bi}_5\text{FeTi}_3\text{O}_{15}$) that allow for an unambiguous choice of a centrosymmetric reference configuration (with space group symmetry $P2_1/m$) for the evaluation of the electric polarization.

In order to model the elastic boundary conditions corresponding to the epitaxial constraint imposed by a substrate, we fix the two short in-plane lattice parameters, a and b , to be equal to an effective substrate lattice constant a' , and the corresponding lattice vectors to form a 90° angle. This corresponds to a thin-film/substrate interface forming a square lattice. Furthermore, for simplicity we constrain the out-of-plane lattice vector to correspond to a perfect base-centered orthorhombic Bravais lattice, in spite of the lower monoclinic symmetry of the whole structure. We find the optimal value of the out-of-plane lattice parameter c (in our notation corresponding to the *conventional* orthorhombic Bravais lattice) by relaxing all ionic positions for fixed a' and different values of c . In the following, whenever comparison with experimental structural data is made, Ref. 8 is used, and we define 0% strain relative to the average experimental in-plane lattice constant $a'_0 = (a^{\text{exp}} + b^{\text{exp}})/2 = 5.45\text{\AA}$.

We perform first-principles calculations using DFT, the projector augmented wave (PAW) method as implemented in the Vienna *ab initio* simulation package (VASP),^{15,16} and the generalized gradient approximation according to Perdew, Burke, and Ernzerhof optimized for solids (PBEsol).¹⁷ Our PAW potentials include 15 valence electrons for Bi ($6s^25d^{10}6p^3$), 14 for Fe ($3p^64s^23d^6$), 10 for Ti ($3p^64s^23d^2$), and 6 for O ($2s^22p^4$). We include a Hubbard “+ U ” correction with $U_{\text{eff}} = 3.0\text{ eV}$ to correctly treat the strong interactions between the Fe d electrons.¹⁸ Ionic positions are relaxed until the residual forces are smaller than 10^{-3} eV/\AA . Calculations are converged using a Γ -centered k -point mesh with $4 \times 4 \times 2$ divisions along the three reciprocal lattice vectors and a plane wave cutoff energy of $E_{\text{cut}} = 550\text{ eV}$. As previously demonstrated,⁹ all magnetic couplings in $\text{Bi}_5\text{FeTi}_3\text{O}_{15}$ are antiferromagnetic, hence we fix antiparallel orientation of the magnetic moments of the two Fe^{3+} cations within the unit cell.

Fig. 2 shows the optimized out-of-plane lattice parameter c as well as the energy of both inner and outer configurations for a range of in-plane lattice parameters a' . The minimum of the energy for each configuration indicates the preferred in-plane lattice parameter for that configuration. Thus, it can be seen that the inner configuration prefers a larger in-plane lattice constant a' than the outer configuration and a shorter out-of-plane lat-

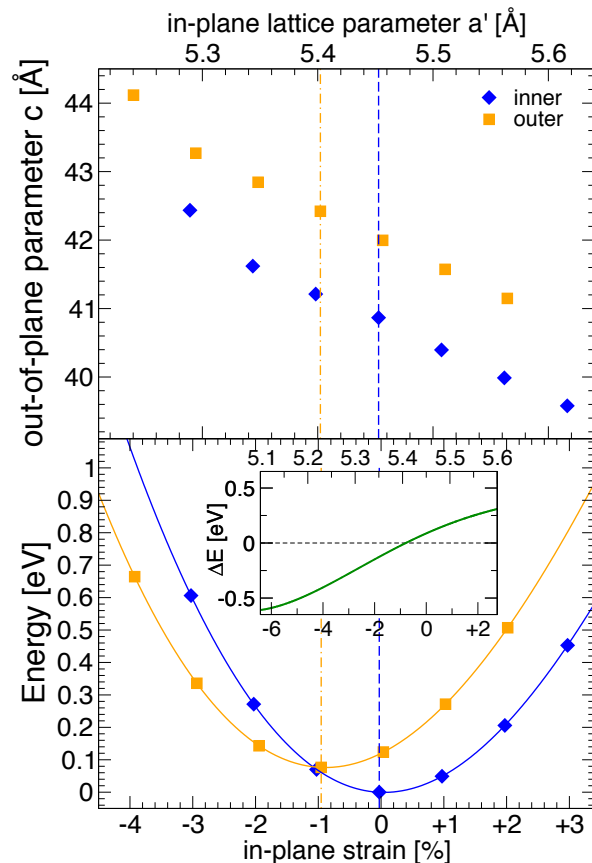


FIG. 2. (Color online) Out-of-plane lattice parameter c (top) and total energy per unit cell (bottom) as a function of in-plane biaxial strain (with the axis at the top of the graph giving the corresponding in-plane lattice parameter), for the inner (blue diamonds) and outer (orange squares) configuration. The dashed lines mark the corresponding equilibrium in-plane parameters for the inner (blue) and outer (orange) configurations, respectively. The inset shows the energy difference ΔE (in eV per cell) between the outer and inner configuration for different values of in-plane strain.

tice parameter c , in agreement with the bulk relaxations presented in Ref. 9. We note that the position of the energy minimum for the inner configuration, i.e., the corresponding preferred in-plane lattice parameter, agrees very well with the averaged experimental in-plane lattice constant, which serves as our zero strain reference. For a given in-plane lattice parameter, the outer configuration always leads to a larger out-of-plane lattice parameter than the inner configuration. This is due to the strong local tetragonality around the Fe^{3+} cation occupying an outer site.⁹ Furthermore, it can be seen that the energy minimum for the inner configuration is lower than the energy minimum for the outer configuration, consistent with the inner site preference of Fe^{3+} found in Ref. 9.

The inner site preference is increased if a' is increased (see Fig. 2, inset). Thus, tensile bi-axial strain is expected to strengthen the inner site preference. On the other hand, when compressive strain is applied, i.e.,

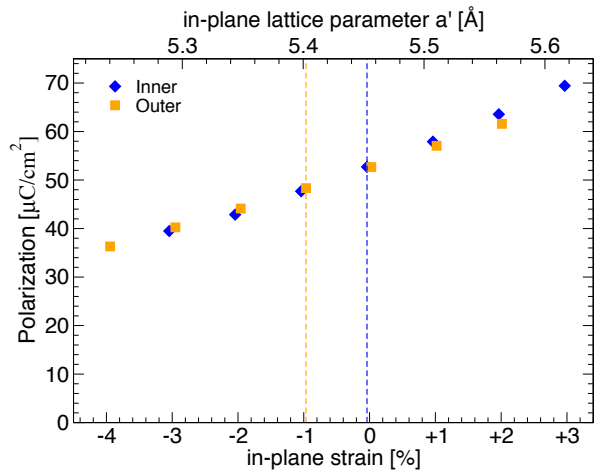


FIG. 3. (Color online) Spontaneous polarization as function of in-plane strain for inner (blue diamonds) and outer (orange squares) configurations. The dashed vertical lines indicate the optimal in-plane lattice parameters for each configuration.

for decreasing a' , the energy difference between inner and outer configuration decreases, and for values below $a' = 5.40$ Å, corresponding to about -1% strain, the outer configuration has a lower energy than the inner configuration.

These results imply that the site preference of the Fe^{3+} cation can indeed be tuned through epitaxial strain. Tensile strain enforces the preference for the inner sites, while compressive strain can reverse this preference such that the majority of Fe^{3+} cations occupy outer sites. We note that these results are obtained by considering only two, albeit representative, configurations, and that a more complete treatment would require to consider more configurations. However, the obtained trend is consistent with the observation from Ref. 9 (and Fig. 2) that outer configurations generally favor a more elongated unit cell (along c) compared to inner ones.

Next, we address the effect of strain on the electric polarization. We calculate the spontaneous polarization P_α along a given direction α using Born Effective Charges (BECs),¹⁹ $Z_{\kappa,\alpha\beta}^*$, as follows

$$P_\alpha = \frac{e}{\Omega} \sum_{\kappa,\beta} Z_{\kappa,\alpha\beta}^* u_{\kappa,\beta} \quad (1)$$

where κ indicates the different ions and $u_{\kappa,\beta}$ is the displacement of ion κ along direction β when going from the paraelectric reference structure to the ferroelectric structure. The BEC tensors are calculated for the polar structures obtained at each strain value using density functional perturbation theory as implemented in VASP.

The calculated polarization as function of strain is depicted in Fig. 3. By symmetry, the polarization is restricted to be aligned along the in-plane two-fold screw axis. At the optimal in-plane lattice constants of either configuration, we find a spontaneous polarization of $P = 48.3 \mu\text{C}/\text{cm}^2$ for the outer configuration, and $P =$

TABLE I. BECs (in units of $|e|$) of the different cations for the two cation distributions in the corresponding centrosymmetric ($P2_1/m$) and polar ($P2_1$) structures. The cations are labeled according to Fig. 1 and separate averages are calculated for the in-plane (xy) and out-of-plane (z) diagonal elements of the BEC tensors.

	inner				outer			
	$P2_1/m$		$P2_1$		$P2_1/m$		$P2_1$	
	xy	z	xy	z	xy	z	xy	z
$\text{Bi}^{3+}(\text{Bi}_2\text{O}_2)$	4.95	4.81	4.81	4.85	5.08	4.51	4.84	4.42
$\text{Bi}^{3+}(\text{perov.})$	5.66	4.08	5.00	4.50	5.76	4.31	5.05	4.49
$\text{Ti}^{4+}(\text{o})$	6.10	6.07	5.97	5.55	4.83	5.71	4.89	5.22
$\text{Ti}^{4+}(\text{i})$	6.48	5.70	5.87	5.66	7.00	5.87	6.20	5.59
$\text{Fe}^{3+}(\text{o})$	—	—	—	—	3.49	4.57	3.55	4.05
$\text{Fe}^{3+}(\text{i})$	4.75	3.90	4.52	3.77	—	—	—	—

$52.7 \mu\text{C}/\text{cm}^2$ for the inner configuration. These results are consistent with the corresponding bulk values from Ref. 9 ($P = 51.5/57.9 \mu\text{C}/\text{cm}^2$ for the outer/inner configuration), calculated using the Berry phase method.²⁰ Note that we are using the BECs calculated for the polar structures to evaluate the spontaneous polarization. Since the BECs decrease when going from the paraelectric to the ferromagnetic structure (see discussion below and Table I), this leads to a small underestimation of the spontaneous polarization compared to the exact calculation of P using the Berry phase.

We observe that in-plane tensile strain leads to a strong increase in polarization and, conversely, compressive strain leads to a strong decrease. The polarization varies by about $\pm 30\%$ over the whole strain region considered here, i.e., from -4% to $+3\%$ strain. This trend is similar to many perovskite ferroelectrics, where an elongation (compression) along the polarization axis increases (decreases) the ferroelectric displacements of the ions, and thus the polarization, along that direction.^{21–23} Similar behavior has also been found in previous DFT studies of the Aurivillius phases $\text{Bi}_4\text{Ti}_3\text{O}_{12}$ ($m = 3$)¹³ and $\text{SrBi}_2\text{Ta}_2\text{O}_9$ ($m = 2$).²⁴

Furthermore, we can see that for a given in-plane lattice parameter, the calculated polarization is very similar for both configurations, in spite of the differences in the out-of-plane lattice parameter c (see Fig. 2). This indicates that the impact of the Fe/Ti distribution on the electric polarization is minimal. The difference in spontaneous polarization obtained for the relaxed inner and outer structures stems mostly from their different in-plane lattice constants ($a' = 5.45$ Å and $a' = 5.40$ Å, respectively). We can conclude that neither does the presence of the magnetic Fe^{3+} cations have a negative impact on the overall magnitude of the electric polarization (compared to, e.g., $\text{Bi}_4\text{Ti}_3\text{O}_{12}$), nor does the specific distribution of magnetic cations have a significant effect on this magnitude.

In order to obtain more detailed insights into the ferro-

electricity of $\text{Bi}_5\text{FeTi}_3\text{O}_{15}$, we now discuss the calculated BECs for different cations in both configurations. Due to the large number of ions and the low symmetry of the system the full results are exhaustive, and we therefore present in Table I only values for the cations, averaged over similar (but not necessarily symmetry-equivalent) sites, calculated for the fully relaxed (i.e., without epitaxial constraint) centrosymmetric and ferroelectric states.

It is apparent that the BECs for both Bi^{3+} and Ti^{4+} (and to some extent also for Fe^{3+}) are highly anomalous, i.e., they are significantly increased compared to the formal valences. This indicates that displacements of the corresponding cations result in large redistribution of charge and corresponding changes in chemical bonding,^{19,25} and is usually considered as a signature for ferroelectrically-active ions.^{26,27} There are no pronounced differences between the two different configurations, except that for the outer configuration the BECs of the $B(o)$ sites are noticeably less anomalous than those of the $B(i)$ sites (and than those of the $B(o)$ sites in the inner configuration). All in all, the BECs for $\text{Bi}_5\text{FeTi}_3\text{O}_{15}$ are similar to the BECs calculated for the related $m = 3$ Aurivillius phase $\text{Bi}_4\text{Ti}_3\text{O}_{12}$ ¹³ and for the related perovskite system (i.e., $m = \infty$) BiFeO_3 .²⁸

One can observe that in most cases (except for the $B(o)$ sites in the outer configuration) the BEC components corresponding to the in-plane directions, i.e., along the polarization direction, are more anomalous than along the out-of-plane direction. Furthermore, the in-plane BECs of Bi^{3+} in the perovskite layer are somewhat more anomalous than those in the Bi_2O_2 layer. A similar trend can be seen in the oxygen BECs (not shown here). Finally, the in-plane BECs in the polar structures are generally reduced compared to the centrosymmetric case, except again for the $B(o)$ sites in the outer configuration.

All these observations suggest that Bi^{3+} , both in the perovskite and in the Bi_2O_2 layers, as well as the B -site Ti^{4+} cations play an active role in driving the polar dis-

placements in this material. However, it is then unclear why the conflicting trends observed for the $B(o)$ sites in the outer configuration would not lead to a more pronounced difference in polarization between the two configurations, which, as pointed out above, is essentially unaffected by the B -site cation distribution (see Fig. 3). Thus, a more detailed study is required to clearly resolve this issue and better understand the origin of ferroelectricity in $\text{Bi}_5\text{FeTi}_3\text{O}_{15}$ and related Aurivillius systems.

To summarize, our calculations indicate that it is indeed possible to control the site preference of the Fe^{3+} cation in $\text{Bi}_5\text{FeTi}_3\text{O}_{15}$ by epitaxial strain. Tensile epitaxial strain is expected to increase the occupation of the inner sites with Fe^{3+} , whereas compressive strain will lead to a preferential Fe^{3+} occupation of outer sites. In addition, epitaxial strain also provides an efficient way to enhance (or reduce) the magnitude of the spontaneous electric polarization, which, furthermore, is rather insensitive to the actual B -site cation distribution.

We point out that the possibility to tailor site preference in $\text{Bi}_5\text{FeTi}_3\text{O}_{15}$ also allows to achieve an essentially homogeneous distribution of Fe^{3+} cations, i.e., no site preference, under moderate compressive strain. This case could indeed be most favorable for achieving good percolation of magnetic couplings between the Fe^{3+} ions and thus promoting long range magnetic order. Therefore, controlling the cation distribution can provide a way of controlling the multiferroic properties of $\text{Bi}_5\text{FeTi}_3\text{O}_{15}$ and related Aurivillius systems.

ACKNOWLEDGMENTS

This work was funded by ETH Zurich and the Swiss National Science Foundation under project no. 200021.141357. We thank Nicoló Fanelli and Rolf Homberger for performing some of the initial calculations for this work as part of their undergraduate research project at ETH Zürich.

* yael.birenbaum@mat.ethz.ch

† claude.ederer@mat.ethz.ch

¹ D. G. Schlom, L.-Q. Chen, X. Pan, A. Schmehl, and M. A. Zurbuchen, *Journal of the American Ceramic Society* **91**, 2429 (2008).

² D. G. Schlom, L.-Q. Chen, C.-B. Eom, K. M. Rabe, S. K. Streiffer, and J.-M. Triscone, *Annual Review of Materials Research* **37**, 589 (2007).

³ K. J. Choi, M. Biegalski, Y. L. Li, A. Sharan, J. Schubert, R. Uecker, P. Reiche, Y. B. Chen, X. Q. Pan, V. Gopalan, L. Q. Chen, D. G. Schlom, and C. B. Eom, *Science* **306**, 1005 (2004).

⁴ J. H. Haeni, P. Irvin, W. Chang, R. Uecker, P. Reiche, Y. L. Li, S. Choudhury, W. Tian, M. E. Hawley, B. Craigo, A. K. Tagantsev, X. Q. Pan, S. K. Streiffer, L. Q. Chen, S. W. Kirchoefer, J. Levy, and D. G. Schlom, *Nature (London)* **430**, 758 (2004).

⁵ S. Bhattacharjee, E. Bousquet, and P. Ghosez, *Phys. Rev. Lett.* **102**, 117602 (2009).

⁶ N. A. Benedek, J. M. Rondinelli, H. Djani, P. Ghosez, and P. Lightfoot, *Dalton Trans.* **44**, 10543 (2015).

⁷ F. Kubel and H. Schmid, *Ferroelectrics* **129**, 101 (1992).

⁸ C. H. Hervoches, A. Snedden, R. Riggs, S. H. Kilcoyne, P. Manuel, and P. Lightfoot, *Journal of Solid State Chemistry* **164**, 280 (2002).

⁹ A. Y. Birenbaum and C. Ederer, *Physical Review B* **90**, 214109 (2014).

¹⁰ R. E. Newnham, R. W. Wolfe, and J. F. Dorrian, *Mat. Res. Bull.* **6**, 1029 (1971).

¹¹ B. Frit and J. P. Mercurio, *Journal of Alloys and Compounds* **188**, 27 (1992).

¹² K. Momma and F. Izumi, *Journal of Applied Crystallography* **44**, 1272 (2011).

¹³ S. H. Shah and P. D. Bristowe, *Journal of Physics-*

- Condensed Matter **22**, 385902 (2010).
- ¹⁴ N. A. Lomanova, V. G. Semenov, V. V. Panchuk, and V. V. Gusarov, *Journal of Alloys and Compounds* **528**, 103 (2012).
- ¹⁵ G. Kresse and J. Furthmüller, *Comput. Mat. Sci.* **6**, 15 (1996).
- ¹⁶ G. Kresse and D. Joubert, *Physical Review B* **59**, 1758 (1999).
- ¹⁷ J. P. Perdew, A. Ruzsinszky, G. Csonka, O. Vydrov, G. Scuseria, L. Constantin, X. Zhou, and K. Burke, *Physical Review Letters* **100**, 136406 (2008).
- ¹⁸ S. L. Dudarev, G. A. Botton, S. Y. Savrasov, C. J. Humphreys, and A. P. Sutton, *Phys. Rev. B* **57**, 1505 (1998).
- ¹⁹ P. Ghosez, J. P. Michenaud, and X. Gonze, *Physical Review B* **58**, 6224 (1998).
- ²⁰ R. D. King-Smith and D. Vanderbilt, *Physical Review B* **47**, 1651 (1993).
- ²¹ C. Bungaro and K. M. Rabe, *Phys. Rev. B* **69**, 184101 (2004).
- ²² O. Diéguez, S. Tinte, A. Antons, C. Bungaro, J. B. Neaton, K. M. Rabe, and D. Vanderbilt, *Phys. Rev. B* **69**, 212101 (2004).
- ²³ C. Ederer and N. A. Spaldin, *Phys. Rev. Lett.* **95**, 257601 (2005).
- ²⁴ Q. Yang, J. X. Cao, Y. Ma, and Y. C. Zhou, *AIP Advances* **3**, 052134 (2013).
- ²⁵ C. Ederer, T. Harris, and R. Kováčik, *Phys. Rev. B* **83**, 054110 (2011).
- ²⁶ M. Posternak, R. Resta, and A. Baldereschi, *Physical Review B* **50**, 8911 (1994).
- ²⁷ K. M. Rabe and P. Ghosez, in *Physics of Ferroelectrics - A modern perspective*, edited by K. Rabe, C. H. Ahn, and J.-M. Triscone (Springer, Berlin/Heidelberg, 2007) pp. 117–174.
- ²⁸ J. B. Neaton, C. Ederer, U. Waghmare, N. A. Spaldin, and K. M. Rabe, *Physical Review B* **71**, 014113 (2005).